Received: 11 March 2022 | Revised: 20 August 2022 | Accepted: 8 November 2022

DOI: 10.4218/etrij.2022-0076

ORIGINAL ARTICLE

ETRI Journal WILEY

Analysis of a nonuniform guiding structure by the adaptive finite-difference and singular value decomposition methods

Abdolshakoor Tamandani[1] | **Mohammad G. H. Alijani**[2]

[1]Faculty of Engineering, Velayat University, Iranshahr, Iran

[2]Electrical Department, Ferdowsi University of Mashhad, Mashhad, Iran

Correspondence
Mohammad G. H. Alijani, Electrical Department, Ferdowsi University of Mashhad, Mashhad, Iran.
Email: malijani@mail.um.ac.ir

Funding information
This research received no external funding.

Abstract

This paper presents a flexible finite-difference technique for analyzing the nonuniform guiding structures. Because the voltage and current variations along the nonuniform structure differ for each segment, this work considers the adaptable discretization steps. This technique increases the accuracy of the final response. Moreover, by applying the singular value decomposition and discarding the nonprincipal singular values, an optimal lower rank approximation of the discretization matrix is obtained. The computational cost of the introduced method is significantly reduced using the optimal discretization matrix. Also, the proposed method can be extended to the nonuniform waveguides. The technique is verified by analyzing several practical transmission lines and waveguides with nonuniform profiles.

KEYWORDS
adaptive finite difference, nonuniform structures, singular value decomposition

1 | INTRODUCTION

Guiding structures with nonuniform profiles are widely used in various applications, including electrical oscillators [1], broadband amplifiers [2], frequency multipliers [3], pulse-shaping devices [4], very large-scale integration interconnectors [5], and wideband antennas [6]. There are two types of nonuniform structures. In the first one, the conductors are not parallel because the transmission lines are crossed over rivers and valleys, or they are parts of structures, such as metallic towers or two-winding transformers. In the second type, the conductors are parallel, but the structure's profile is not uniform, such as in exponential impedance-matching networks and stepped impedance microstrip filters [7–9].

Several analytical solutions have been introduced for analyzing specific cases, such as structures with exponential [10], linearly tapered [11], power-law [12], and Hermit [13] profiles. Except for the nonuniform structures with a few special profiles, no analytical modeling with the general profiles has been introduced. Also, numerous numerical-based techniques are presented for studying nonuniform guiding structures. However, their disadvantages include high computational cost, slow convergence, high required time, hard to implement, and hard to generalize.

This work introduces a new technique based on the flexible finite-difference method for analyzing the nonuniform guiding structures. Therefore, adaptable discretization steps are used for each segment to increase the final response's accuracy. This method can determine the magnitude and phase of the voltage and current and the scattering parameters of a nonuniform structure. Furthermore, the singular value decomposition is used to reduce the computational cost. The introduced method is straightforward to implement, accurate, and faster than

the traditional approaches based on the discretization technique. The method can be easily extended to the nonuniform waveguide in its dominant mode.

2 | THEORY AND FORMULATION

Figure 1 shows a nonuniform structure with a general profile. This structure conveys transverse electromagnetic (TEM) or quasi-TEM waves. Therefore, the following differential equations describe the structure's voltage $V(x)$ and current $I(x)$, where $Z(x)$ and $Y(x)$ are the per unit length impedance and admittance, respectively [14].

$$dV/dx = -Z(x)I(x), \tag{1}$$

$$dI/dx = -Y(x)V(x). \tag{2}$$

The per unit length parameters vary along the line. The above differential equations' analytical solutions cannot be easily found. A solution to a problem with an excellent approximation can be obtained using the discretization theory if the step size is sufficiently small. In other words, the problem's differential equations can be converted into a finite-dimensional matrix expression using the discretization theory. Therefore, the voltage and current derivatives at any point x_n are estimated using the forward-difference formula [15].

$$\frac{dV}{dx}_{x=x_n} \approx \frac{V(x_n+h)-V(x_n)}{h_n^v}, \tag{3}$$

$$\frac{dI}{dx}_{x=x_n} \approx \frac{I(x_n+h)-I(x_n)}{h_n^i}, \tag{4}$$

where ${h_n}^v$ and ${h_n}^i$ are the voltage and current step sizes, respectively. The voltage and current step sizes ${h_n}^v$ and ${h_n}^i$ are constant in the conventional finite-difference method. Because a nonuniform structure's voltage and current variations might be sharp in some intervals and smooth in others, the steps ${h_n}^v$ and ${h_n}^i$ with constant values are not good candidates. Therefore, this work considers adjustable steps. In other words, the values of ${h_n}^v$ and ${h_n}^i$, where the voltage or current interval variations are sharp, differ from the others. Hence, their value should be determined smartly. Note that the values of ${h_n}^v$ and ${h_n}^i$ are still unknown. Later, more details about the step size selection will be presented.

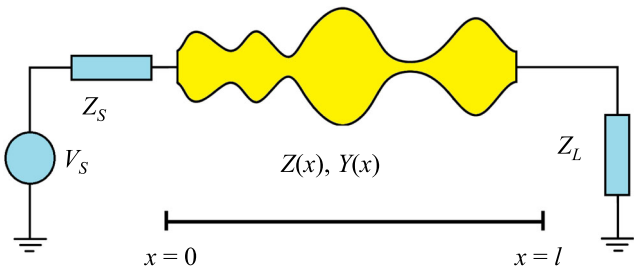

FIGURE 1 The general scheme of a nonuniform structure

It is assumed that the interval $0 \le x \le l$ is divided into $N+1$ segments as $x_1 = 0 \le x_n \le x_{N+1} = l$. Substituting (3) and (4) into (1) and (2) provides the following equations, where $n = 1, 1, \ldots, N$, $V_n = V(x_n)$, $I_n = I(x_n)$, $Z_n = Z(x_n)$, and $Y_n = Y(x_n)$.

$$V_n - V_{n+1} - h_n^v Z_n I_n = 0, \tag{5}$$

$$I_n - I_{n+1} - h_n^i Y_n V_n = 0. \tag{6}$$

Also, the boundary conditions at the two terminals are

$$V_1 = V_S - Z_S I_1 \quad \text{and} \tag{7}$$

$$V_{N+1} = Z_L I_{N+1}. \tag{8}$$

Equations (5), (6) and (7), (8) can be expressed in a matrix form as

$$\mathbf{AX} = \mathbf{B} \rightarrow \mathbf{X} = \mathbf{A}^{-1}\mathbf{B}, \tag{9}$$

where

$$\mathbf{X} = [\mathbf{V}\ \mathbf{I}]^{\mathrm{T}}, \tag{10a}$$

$$\mathbf{V} = [V_1 \ \cdots \ V_{N+1}], \tag{10b}$$

$$\mathbf{I} = [I_1 \ \cdots \ I_{N+1}], \tag{10c}$$

$$\mathbf{B} = [V_S \ 0 \ \cdots \ 0]^{\mathrm{T}}_{1\times(2N+2)}, \tag{11}$$

$$\mathbf{A} = \begin{bmatrix} \mathbf{A}_{11} & \mathbf{A}_{12} \\ \mathbf{A}_{21} & \mathbf{A}_{22} \end{bmatrix}_{(2N+2)\times(2N+2)}. \tag{12}$$

The discretization matrix $\mathbf{A}$ is constructed from four blocks as follows.

$$\mathbf{A}_{11} = \begin{bmatrix} 1 & 0 & 0 & 0 & \cdots & 0 \\ 1 & -1 & 0 & 0 & \cdots & 0 \\ 0 & 1 & -1 & 0 & \cdots & 0 \\ \vdots & \vdots & \vdots & \vdots & \cdots & \vdots \\ 0 & \cdots & 0 & 1 & -1 & 0 \\ 0 & \cdots & 0 & 0 & 1 & -1 \end{bmatrix}, \tag{13a}$$

$$\mathbf{A}_{12}=\begin{bmatrix} Z_S & 0 & \cdots & 0 \\ -h_1^v Z_1 & 0 & \cdots & 0 \\ 0 & -h_2^v Z_2 & \ddots & \vdots \\ \vdots & \ddots & \ddots & 0 \\ 0 & \cdots & 0 & -h_N^v Z_N \end{bmatrix}, \tag{13b}$$

$$\mathbf{A}_{21}=\begin{bmatrix} -h_1^i Y_1 & 0 & \cdots & 0 \\ 0 & \ddots & \ddots & \vdots \\ \vdots & \ddots & -h_N^i Y_N & 0 \\ 0 & \cdots & 0 & 0 \\ 0 & \cdots & 0 & 1 \end{bmatrix}, \tag{13c}$$

$$\mathbf{A}_{22}=\begin{bmatrix} 1 & -1 & 0 & 0 & \cdots & 0 \\ 0 & 1 & -1 & 0 & \cdots & 0 \\ 0 & 0 & 1 & -1 & \cdots & 0 \\ \vdots & \vdots & \vdots & \vdots & \cdots & \vdots \\ 0 & \cdots & 0 & 0 & 1 & -1 \\ 0 & \cdots & 0 & 0 & 0 & -Z_L \end{bmatrix}. \tag{13d}$$

The first row of $\mathbf{A}_{11}$ and $\mathbf{A}_{12}$ and the last row of $\mathbf{A}_{21}$ and $\mathbf{A}_{22}$ include the boundary conditions.

Truncation or discretization errors are crucial in this method and should be reduced. Reducing the values of $h_n{}^v$ and $h_n{}^i$ will increase accuracy. Moreover, reducing the values could increase the round-off error [16]. The values of $h_n{}^v$ and $h_n{}^i$ have three suggestions: the large step $h_n{}^v$, $h_n{}^i \le \lambda/10$, the middle step $h_n{}^v$, $h_n{}^i \le \lambda/20$, and the small step $h_n{}^v$, $h_n{}^i \le \lambda/40$, where λ is the wavelength corresponding to the highest frequency [16]. Although $h_n{}^v$, $h_n{}^i \le \lambda/40$ produces the least truncation error compared to the others, it increases the round-off error and computational cost. Therefore, the matrix approximation lemma or Eckart–Young–Mirsky theorem is used. The singular value decomposition of matrix $\mathbf{A}$ is first calculated as [17]

$$\mathbf{A}=\mathbf{U}\mathbf{S}\mathbf{V}^{\mathrm{T}}, \tag{14}$$

where

$$\mathbf{U}^{\mathrm{T}}\mathbf{U}=\mathbf{1}, \tag{15}$$

$$\mathbf{V}^{\mathrm{T}}\mathbf{V}=\mathbf{1}, \tag{16}$$

where $\mathbf{1}$ and $\mathbf{S}$ show the identity and diagonal matrixes containing the singular values of $\mathbf{A}$ in decreasing order on its diagonal. Also, the columns of $\mathbf{U}$ are the left singular vectors, and the rows of $\mathbf{V}$ are the right singular vectors. Moreover, the singular values in $\mathbf{S}$ are square roots of the eigenvalues of $\mathbf{A}\mathbf{A}^{\mathrm{T}}$. Our studies show that some singular values are nearly zero for practical applications. Therefore, the nonprincipal singular values can be discarded. From this, a low-rank approximation of the coefficient matrix $\mathbf{A}$ is determined as [17]

$$\mathbf{A}_Q=\mathbf{U}\mathbf{S}_Q\mathbf{V}^{\mathrm{T}}, \tag{17}$$

where $\mathbf{A}_Q$ and $\mathbf{S}_Q$ are the low-rank and diagonal matrixes containing the principal singular values of $\mathbf{A}$, respectively. It is assumed that the single values of matrixes $\mathbf{A}$ and $\mathbf{A}_Q$ are M and Q, respectively, where $Q < M$. By the low-rank coefficient matrix $\mathbf{A}_Q$, the problem's round-off error and computational cost will decrease significantly. Therefore, without worrying about the round-off error and computational cost, the values of $h_n{}^v$ and $h_n{}^i$ can be reduced to increase the final solution's accuracy.

The proper selection of $h_n{}^v$ and $h_n{}^i$ is essential. Therefore, we consider the updated version of (3) and (4) as

$$\frac{dV}{dx}\approx\frac{V(x_n+h)-V(x_n)}{h_n^v}+E_v\left(h_n^v,x_n\right) \text{ and} \tag{18}$$

$$\frac{dI}{dx}\approx\frac{I(x_n+h)-I(x_n)}{h_n^i}+E_i\left(h_n^i,x_n\right), \tag{19}$$

where $E_v\,(h_n{}^v, x_n)$ and $E_i\,(h_n{}^v, x_n)$ are the voltage and current truncation errors, respectively. An iterative technique is regarded to obtain the minimum error. Therefore, it is assumed that $h_n{}^v$ and $h_n{}^i$ are constant. Then, the voltage and current are computed. The closed-form expression of the computed voltage and current are calculated using the Fourier series as

$$V(x)=\sum_n v_n\exp(jn\gamma x) \text{ and} \tag{20}$$

$$I(x)=\sum_n i_n\exp(jn\gamma x), \tag{21}$$

where v_n and i_n are the voltage and current Fourier coefficients, respectively. Also, γ is the propagation constant of the TEM mode propagating on the line. Note that the Fourier coefficients v_n and i_n are easily calculated, as described in [18]. Substituting the general terms of (20) and (21) into (18) and (19) gives

$$E_v = \sum_n v_n \left\{ \gamma_n - \left(e^{\gamma_n h_n^v} - 1 \right) / h_n^v \right\} e^{\gamma_n x_n} \quad \text{and} \tag{22}$$

$$E_i = \sum_n i_n \left\{ \gamma_n - \left(e^{\gamma_n h_n^i} - 1 \right) / h_n^i \right\} e^{\gamma_n x_n}. \tag{23}$$

If the calculated error for each point (x_n) is unacceptable, the values of $h_n{}^v$ and $h_n{}^i$ should be updated as

$$h_n^v, h_n^i = (\lambda/20)(1 - t/2T), \tag{24}$$

where $E_i{}^d$ and $E_v{}^d$ are the current and voltage desired error defined by the designer. Also, $t = 1, 2, ..., T$, where T is the total number of iterations and λ is the wavelength corresponding to the highest frequency. In the above equations, it is assumed that the step size variation intervals are $\lambda/40 \le h_n{}^v \le \lambda/20$, $\lambda/40 \le h_n{}^i \le \lambda/20$. Our studies show that for the practical structures, only two or three iterations are sufficient to obtain an answer with excellent accuracy. Figure 2 shows the flowchart of the proposed procedure.

The scattering parameters are required instead of the voltage and current for microwave applications. Therefore, the introduced equations in [19] can be used after determining the voltage and current. Note that for the symmetrical and reciprocal structures, $S_{11} = S_{22}$, $S_{12} = S_{21}$, and according to the conservation of the power principle, $|S_{11}|^2 + |S_{21}|^2 = 1$ [14].

Equation (13) shows that the final solution's accuracy depends on $Z(x)$ and $Y(x)$. There is no closed-form expression for most practical nonuniform structures, and the numerical techniques should be used to compute $Z(x)$ and $Y(x)$ [20].

The proposed technique can be easily developed for a nonuniform waveguide operating in its dominant mode. Here, the electric and magnetic fields have only one component. It is shown in [21] that the waveguide's dominant mode has a characteristic field pattern across any section of the waveguide structure. Therefore, the amplitude variations of the electric and magnetic fields along the waveguide can be modeled by the currents and voltages, satisfying the transmission line equations as

$$dV/dx = (j\eta\beta^2/k) I \quad \text{and} \tag{25a}$$

$$dI/dx = (jk/\eta) V, \tag{25b}$$

where

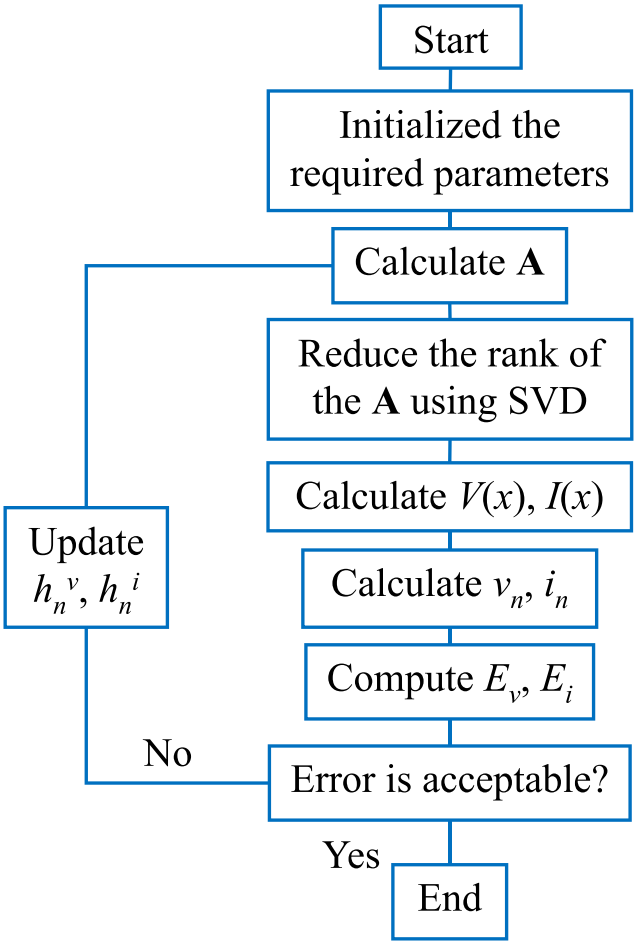

FIGURE 2 The flowchart of the proposed procedure

$$k = \omega\sqrt{\mu\varepsilon}, \eta = \sqrt{\mu/\varepsilon}, \tag{26}$$

where β is the propagation constant. Note that the above equations are only valid for a uniform waveguide. As shown in Equation (13), only $Z(x)$ and $Y(x)$ are needed for analyzing a nonuniform waveguide. The per unit length impedance and admittance of a rectangular waveguide with a nonuniform profile in the dominant mode TE_{10} can be found in [11].

$$Z(x) = j\omega\mu h / w(x), \tag{27a}$$

$$Y(x) = j\gamma^2(x) w(x) / \omega\mu h, \quad \text{and} \tag{27b}$$

$$\gamma(x) = \sqrt{k^2 - (\pi/w(x))^2}, \tag{27c}$$

where h, $w(x)$, and $\tan\delta$ are the waveguide's height and width and the dielectric loss tangent, respectively. Now, by specifying $Z(x)$ and $Y(x)$, the waveguide's voltage,

current, and scattering parameters can be determined. For other types of waveguides, a similar procedure can be applied.

3 | RESULTS AND DISCUSSIONS

This section examines several theoretical and practical TLs and waveguides with nonuniform profiles to evaluate the proposed approach's performance. For the practical examples, the results are compared to those obtained from simulations (using HFSS software), measurements, and the Uniform Cascaded Section (UCS) method [20].

3.1 | Uniform transmission line

In the first case, a uniform TL line is considered, with parameters $L_0 = 0.33$ μH/m, $C_0 = 33.33$ pF/m, $R_0 = 2$ Ω/m, $G_0 = 0.2$S/m, $l = 20$ mm, $V_S = 1$ v, $Z_L = 100$ Ω, and $Z_S = 50$ Ω. The exact solution of the uniform TL can be found in [18]. Figure 3 compares the magnitude and phase of the calculated voltage and current versus frequency and position from the exact formulas and the proposed method, respectively. There is excellent agreement between the results of the proposed and theoretical approaches.

3.2 | Catenary transmission line

The catenary TL is frequently used in power systems, including high-voltage overhead lines and electrified railways. In the second case, a catenary TL with the following profile is considered [22].

$$y(x) = q\cosh(x/q - l/2q). \tag{28}$$

The per unit length impedance and admittance of a catenary TL are calculated as

$$Z(x) = (j\omega\mu/2\pi)\cosh^{-1}(2y(x)/r_0) \text{ and} \tag{29a}$$

$$Y(x) = j2\pi\omega\varepsilon/\cosh^{-1}(2y(x)/r_0), \tag{29b}$$

where $q = 2$, $l = 1$ m, and $r_0 = 1$ mm are the parameters of the line and $V_S = 1$ v, $Z_L = 75\ \Omega$, and $Z_S = 50$. Figure 4 shows that the propagation constant is not a function of x, and $\gamma^2 = Z(x)Y(x) = \text{cte}$.

Note that there is no exact solution for the catenary TL. Figure 5 shows the magnitude and phase of the calculated voltage and current versus frequency and position from the proposed and TMM methods in [23]. There is excellent agreement between the results of the proposed and theoretical approaches. These figures show excellent agreement between the results.

3.3 | Nonuniform microstrip line

The microstrip lines with nonuniform profiles are used in microwave circuits as resonators and filters. In [24], a low-pass filter is designed using the nonuniform microstrip line with parameters of $\varepsilon_r = 3.5$, $H = 768$ μm, and $l = 10$ cm. Two filter ports are terminated with 50 Ω

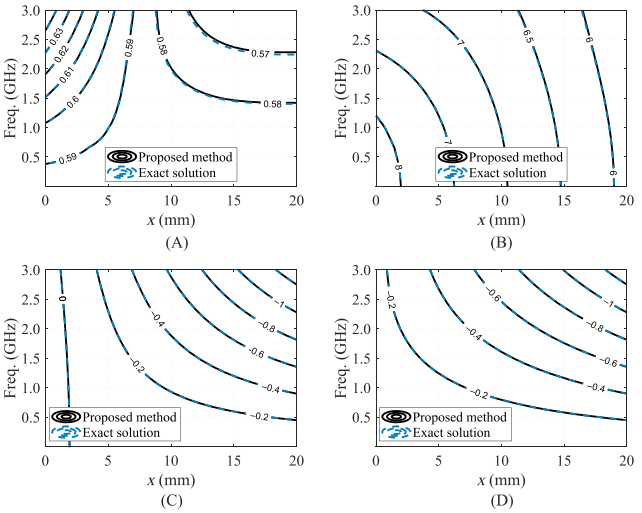

FIGURE 3 Comparison between the proposed method and the exact solution of V and I of a single uniform TL (A)$|V|(v)$, (B)$|I|$ (mA), (C) $\angle V$ (rad), (D) $\angle I$ (rad)

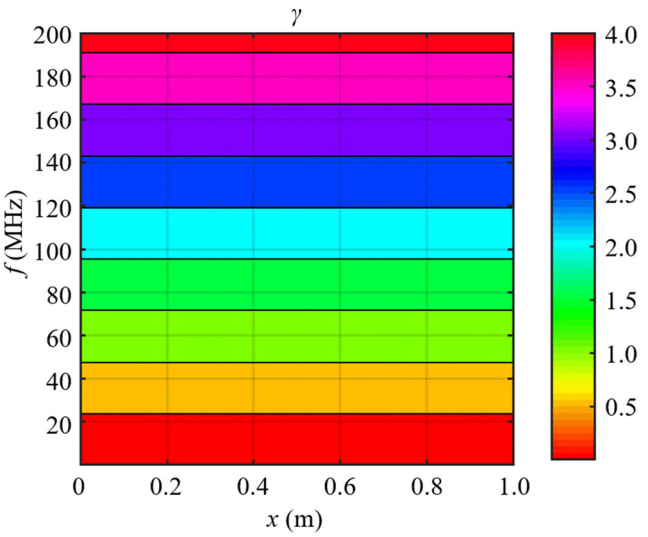

FIGURE 4 The propagation constant of the catenary TL

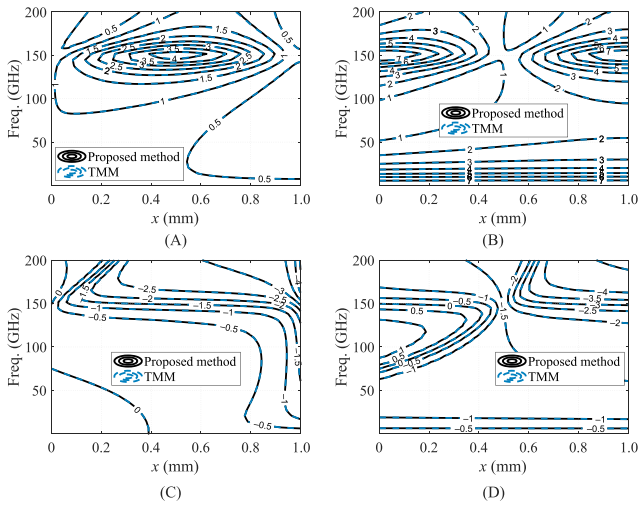

FIGURE 5 Comparison between the proposed method and the exact solution of V and I of the catenary TL: (A)$|V|(v)$, (B)$|I|$ (mA), (C) $\angle V$ (rad), (D) $\angle I$ (rad)

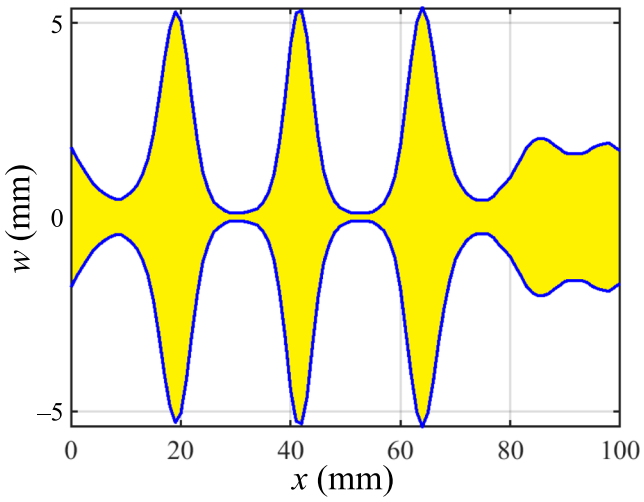

FIGURE 6 The profile of the low-pass filter with nonuniform microstrip line

impedance. Figure 6 shows the strip's width as a function of x. Figure 7 compares the response of the filter obtained from the proposed method with those obtained from simulations, measurements, and the UCS method. The introduced technique and other data correlate well.

3.4 | Nonuniform TL with sharp discontinuities

A nonuniform TL with sharp discontinuities is used for various applications such as filters. A microstrip TL with

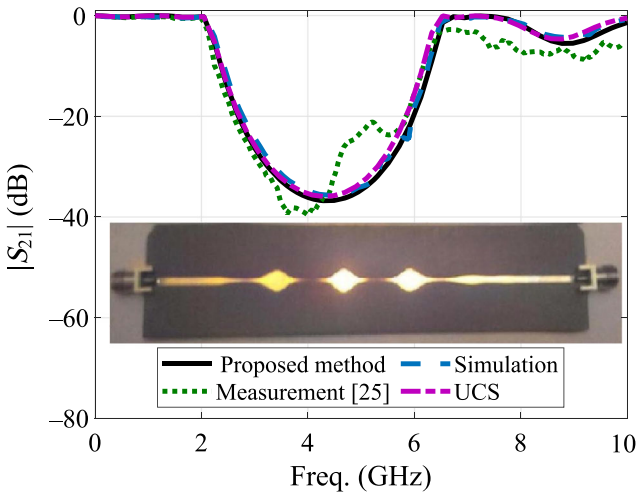

FIGURE 7 The response of the microstrip filter with a nonuniform profile

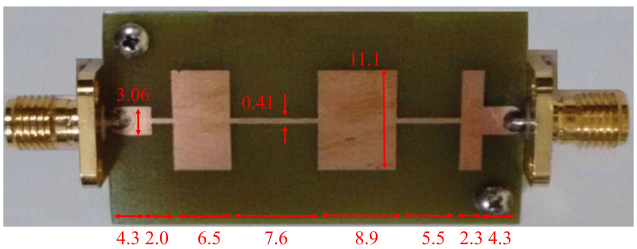

FIGURE 8 The photo of the fabricated stepped filter with dimensions in mm [25]

a stepped profile is considered the fourth case. The structure's parameters are $\varepsilon_r = 4.4$, $\tan\delta = 0.02$, $H = 1.6$ mm, and $Z_S = Z_L = 50\ \Omega$. This structure comprises six steps, where the widths of the highest and lowest steps are 11.1 and 0.4080 mm, respectively. Figure 8 shows the fabricated filter with dimensions. Figures 9 and 10 show the structure's scattering parameters, including the obtained results of the proposed method, simulations, measurements [25], and the UCS technique in the frequency range of 0 to 5 GHz. For the magnitude of S_{11}, there is a difference of approximately 10 dB between the results of the proposed method and simulation/measurement data at lower frequencies, which is also true for the UCS technique's results. The mismatch between the results is due to the connector effect, which is excluded in the proposed and UCS procedures. Additionally, as stated in [14], the higher order modes will appear around the discontinuities position, which are disregarded in the proposed and UCS techniques. However, both techniques' accuracy are acceptable. For the magnitude of S_{21}, the proposed

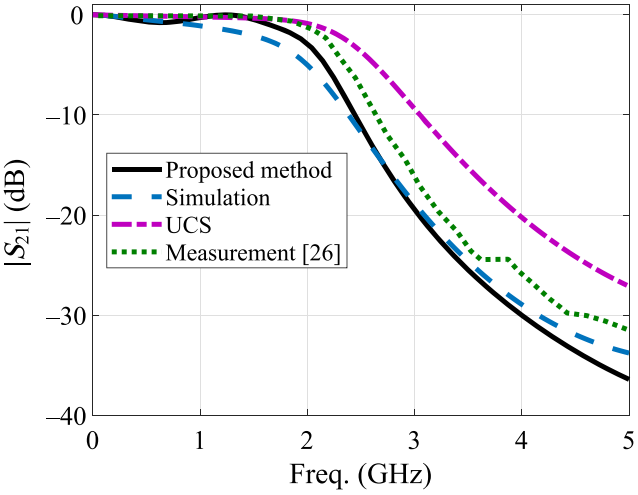

FIGURE 9 Magnitude of S_{11} of the stepped impedance filter

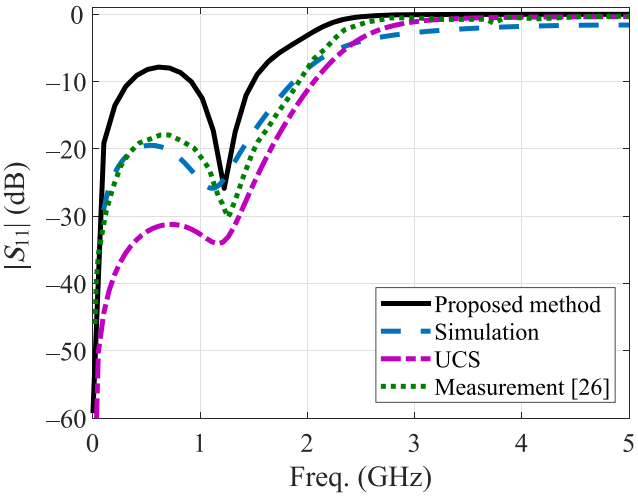

FIGURE 10 Magnitude of S_{21} of the stepped impedance filter

method's accuracy is higher than the UCS technique at all frequencies.

3.5 | Nonuniform substrate-integrated waveguide (SIW)

The introduced technique can also analyze a nonuniform waveguide operating in its dominant mode. A double-slop linearly tapered SIW operating in a fundamental TE_{10} mode is considered in the fifth case. Figure 11 shows that the parameters of this structure are $\varepsilon_r = 3.66$, $\tan\delta = 0.0037$, $H = 254$ μm, $l = 44$ mm, and $Z_S = Z_L = 50\ \Omega$. In the SIW structure, the width of an equivalent rectangular waveguide section is determined as [11]

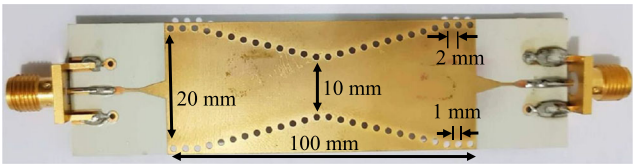

FIGURE 11 The photo of fabricate nonuniform SIW [11]

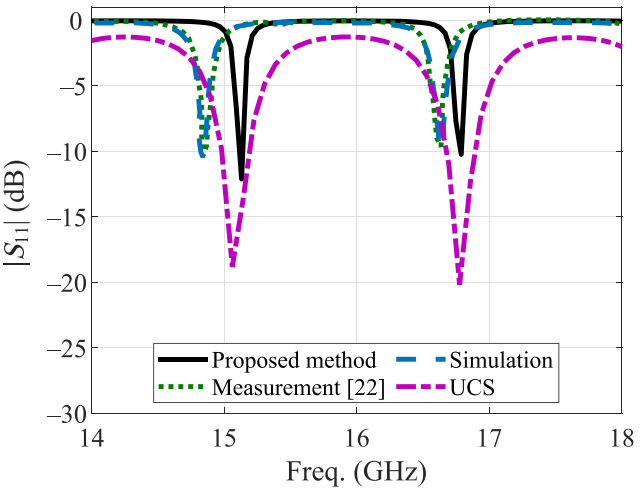

FIGURE 12 Magnitude of S_{11} of the SIW structure

$$W_{\text{eff}} = W\left(a_1 + \frac{a_2}{S/d + (a_1 + a_2 - a_3)/(a_3 - a_1)}\right), \quad (30a)$$

$$a_1 = 1.019 + 0.346/(W/S - 1.068), \quad (30b)$$

$$a_2 = -0.118 + 1.272/(W/S - 1.201), \text{ and} \quad (30c)$$

$$a_3 = 1.008 + 0.916/(W/S + 0.215), \quad (30d)$$

where W is the physical width of the SIW. The SIW's per unit length parameters are calculated using the closed-form formulas introduced in [26]. The structure's scattering parameters are plotted in Figures 12 and 13, including the obtained results of the proposed method, simulations, measurements [11], and the UCS technique in the frequency range of 14 GHz to 18 GHz. The UCS method's performance is not good because, in general, the UCS technique cannot be applied to a nonuniform waveguide. The slight frequency shift is approximately 0.18 GHz over the frequency range of 14 GHz to 18 GHz and is due to the transition between the SIW and Sub-Miniature version A (SMA) connectors and the fabrication imperfections, which are not regarded in the proposed method.

The mentioned conditions cause a peak magnitude deviation of approximately 4 dB, especially at resonance

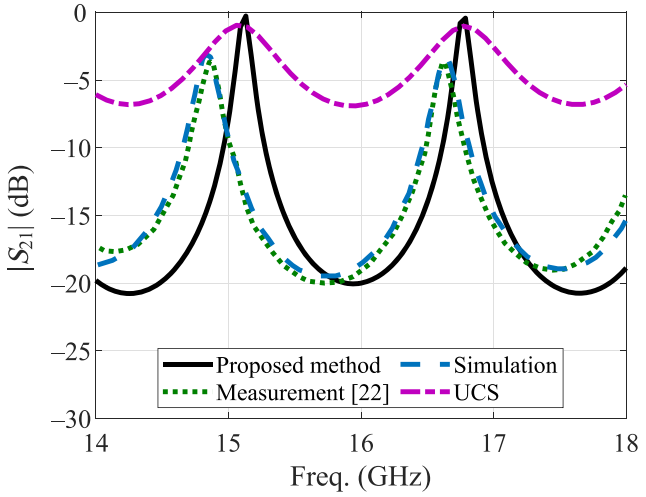

FIGURE 13 Magnitude of S_{21} of the SIW structure

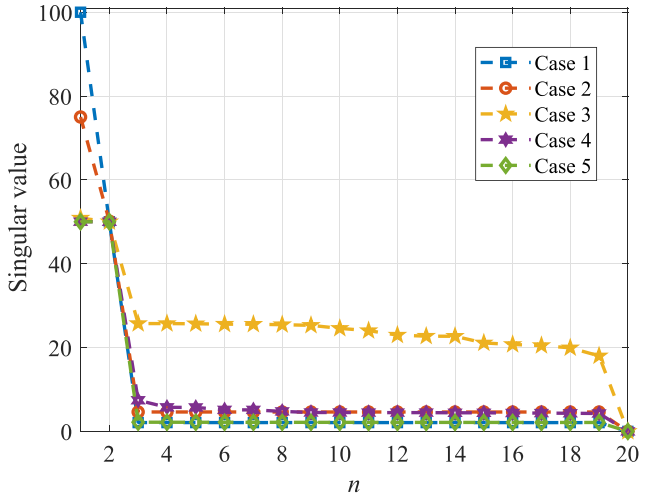

FIGURE 14 The most crucial singular values of all studied cases

frequencies. However, the precision of the obtained results is acceptable over a wide frequency range.

Figure 14 shows all studied examples' most crucial singular values. By ignoring the coefficient matrix's non-principal singular values, the round-off error and the computational cost will significantly decrease. The figure shows that most of the singular values of the lower rank coefficient matrix $\mathbf{A}_Q$ are on the same level.

Table 1 reports the crucial parameters of all cases, including the required time t, number of segments N, total number of iterations T, and condition number of the coefficient matrix τ. Note that the condition number measures a problem's sensitivity [27]. The condition number of all examined cases is in an acceptable range. Therefore, the proposed method's sensitivity is low regarding the discretization error. Also, for all studied

TABLE 1 Comparison of the crucial parameters of all studied cases.

	t (s)	N	T	τ
Case 1	6.4	300	1	1.0×10^6
Case 2	0.7	100	2	2.1×10^6
Case 3	3.5	100	2	3.1×10^6
Case 4	2.6	100	2	3.1×10^4
Case 5	23.0	300	1	3.9×10^4

cases, only one or two iterations are sufficient to obtain an answer with excellent accuracy. Moreover, the proposed method uses a PC with a CPU core i5 @2.3GHz and 4G RAM. The required running time shows that the method is computationally inexpensive.

4 | CONCLUSIONS

This article introduced a new technique based on the flexible finite-difference method to analyze nonuniform transmission lines and waveguides. Therefore, adjustable discretization steps are employed for each segment to increase the final outcome's accuracy. The method can calculate the voltage and current values, including the magnitude and phase and the scattering parameters of a nonuniform guiding structure. Additionally, the singular value decomposition is used to reduce the computational complexity. The method is straightforward to implement, accurate, and faster than the traditional discretization techniques. The proposed approach's performance is confirmed by analyzing several practical transmission lines and waveguides with nonuniform profiles.

CONFLICT OF INTEREST STATEMENT

The authors declare that there are no conflicts of interest.

ORCID

Mohammad G. H. Alijani https://orcid.org/0000-0002-8143-9247

REFERENCES

1. H. Cho, M. Go, Y. Jo, and H. Park, *Oscillator with high harmonic suppression using split quarterwave microstrip resonator*, ETRI J. **33** (2011), 125–127.
2. M. Fernandez, S. Ver Hoeye, C. Vazquez, L. Alonso Gonzalez, and F. Las-Heras, *On the design of broadband hybrid amplifiers using nonuniform transmission lines as impedance matching networks*, IEEE Access **7** (2019), 19670–19677.
3. M. Adnan and E. Afshari, *Efficient microwave and millimeter-wave frequency multipliers using nonlinear transmission lines in CMOS technology*, IEEE Trans. Microw. Theory Technique **63** (2015), no. 9, 2889–2896.

4. P. Rulikowski and J. Barrett, *Ultra-wideband pulse shaping using Lossy and dispersive nonuniform transmission lines*, IEEE Trans. Microw. Theory Techniques **59** (2011), no. 10, 2431–2440.
5. A. Cheldavi and D. Ansari, *Efficient frequency-domain modelling and simulation of nonuniform coupled transmission lines: Application in transient analysis of VLSI circuits*, Can. J. Elect. Comput. Eng. **29** (2004), no. 3, 167–177.
6. R. Wu and Q.-X. Chu, *Broadband multimode antenna and its array for wireless communication base stations*, ETRI J. **41** (2019), 167–175.
7. F. Khajeh-Khalili and M. A. Honarvar, *Novel tunable peace-logo planar metamaterial unit-cell for millimeter-wave applications*, ETRI J. **40** (2018), 389–395.
8. S. H. Kazemi, M. Ghanbarpour, A. Zahedi, and M. Hayati, *A microstrip lowpass filter with sharp roll-off using arrow-shaped resonators and high-impedance open stubs*, AEU-Int. J. Electron. C. **136** (2021), 1–8.
9. S. M. S. N. Hosseini, R. Zaker, and K. Monfaredi, *A microstrip folded compact wideband band-pass filter with wide upper stop-band*, ETRI J. **43** (2021), 957–965.
10. F. Vega, F. Rachidi, N. Mora, N. Pena, and F. Roman, *Design, realization, and experimental test of a coaxial exponential transmission line adaptor for a half-impulse radiating antenna*, IEEE Trans. Plasma Sci. **41** (2013), no. 1, 173–181.
11. K. Rabaani, M. Added, N. Boulejfen, A. B. Kouki, and F. M. Ghannouchi, *Chebyshev polynomials for the numerical modeling of non-uniform substrate integrated waveguides*, Int. J. Numer. Modell. Electron. Netw. Devices Fields **34** (2020), no. 3, 1–15.
12. A. Cheldavi, *Exact analysis of coupled nonuniform transmission lines with exponential power law characteristic impedance*, IEEE Trans. Microw. Theory Techniques **49** (2001), no. 1, 197–199.
13. A. Cheldavi, *Analysis of coupled Hermite transmission lines*, IEE Proc. Microw. Antennas Propag. **150** (2003), no. 4, 279–284.
14. D. M. Pozar, *Microwave engineering*, John Wiley & Sons, 2011.
15. S. C. Chapra, *Applied numerical methods; with MATLAB for engineers and scientists*, MC Graw Hill, 2015.
16. M. N. O. Sadiku, *Numerical techniques in electromagnetics with MATLAB*, CRC Press, 2018.
17. K. Kanatani, *Linear algebra for pattern processing: Projection, singular value decomposition, and pseudoinverse*, Morgan & Claypool, 2021.
18. A. Gilat and V. Subramaniam, *Numerical methods for engineers and scientists*, John Wiley & Sons, 2014.
19. P. A. Rizzi, *Microwave engineering; passive circuits*, Prentice-Hall, 1988.
20. C. R. Paul, *Analysis of multiconductor transmission lines*, 2nd ed., John Wiley & Sons, 2008.
21. K. A. Milton and J. Schwinger, *Electromagnetic radiation: Variational methods, waveguides and accelerators*, Springer, 2006.
22. L. L. Grigsby, *The electric power engineering handbook; electric power generation, transmission, and distribution*, CRC Press, 2012.
23. J. A. B. Faria, *The transfer matrix method: Analysis of nonuniform multiport systems*, IEEE Access **8** (2020), 23650–23662.
24. M. Khalaj-Amirhosseini and S. A. Akbarzadeh-Jahromi, *To optimally design microstrip nonuniform transmission lines as lowpass filters*, J. Telecommun. **2** (2010), no. 2, 139–142.
25. S. Das and S. K. Chowdhury, *Design simulation and fabrication of stepped impedance microstrip line low pass filter for S-band application using IE3D and MATLAB*, Int. J. Electron. Commun. Technol. **3** (2012), no. 1, 98–100.
26. M. Alijani Ghadikolae and M. H. Neshati, *Development an accurate and simple dispersion analysis of TE10 mode of substrate integrated waveguide*, *(21st Iranian conference on electrical engineering (ICEE), Mashhad, Iran)*, 2013, pp. 1–4.
27. G. Strang, *Introduction to linear algebra*, Cambridge Press, 2016.

AUTHOR BIOGRAPHIES

Abdolshakoor Tamandani was born in Khash, Iran, in 1987. He received the B.Sc. degree in Electrical Engineering from the Chabahar Maritime University, Chabahar, Iran, in 2010 and the M.Sc. degree in Electrical Engineering from the Sistan and Baluchestan University, Zahedan, Iran, in 2012. He is currently a lecturer with the Electrical Engineering Department, Velayat University of Iranshahr, Iran. His research interests include design and analysis of RF and microwave components, circuits, antennas, and metamaterials.

Mohammad G. H. Alijani was born in Mazandaran, Iran. He received a Ph.D. degree in electrical engineering from Ferdowsi University of Mashhad, Mashhad, Iran, in 2019. He was a visiting researcher with the EMC Group, Politecnico di Torino, Torino, Italy, in 2019-2020. He has published over 20 journal articles, conference papers, and patents. He is a coauthor of two books. Also, he is a member of the National Elite Foundation of Iran. He is currently a reviewer of the IEEE Transaction on Electromagnetic Compatibility, International Journal of Electronics and communications, AEU, and International Journal of Engineering. His research interests include electromagnetic theory, microwave and antenna theory, design, EMC, and application of machine learning in applied electromagnetic.

How to cite this article: A. Tamandani and M. G. H. Alijani, *Analysis of a nonuniform guiding structure by the adaptive finite-difference and singular value decomposition methods*, ETRI Journal **45** (2023), 704–712. https://doi.org/10.4218/etrij.2022-0076